

## Use of different X-ray tomographic systems for cultural-heritage samples

A. BRUNETTI

*Struttura Dipartimentale di Matematica e Fisica, Università di Sassari  
Via Vienna 2, 07100, Sassari, Italy  
INFN, Sezione di Cagliari - Cagliari, Italy*

(ricevuto il 10 Novembre 2006; revisionato il 27 Febbraio 2007; approvato l'1 Marzo 2007; pubblicato online il 5 Giugno 2007)

**Summary.** — X-ray tomography is a well-known non-destructive form of testing. Internal parts of a sample may be analysed without destroying them. This is important for several reasons. First, the overall state of conservation of the manufacts can be determined. Otherwise it would be based only on the external surface state. Secondly, the manufacturing techniques can be identified and thirdly, a more precise plan of restoration can be decided upon. In this paper the X-ray tomography principles are described and the principal applications of this technique to cultural-heritage samples reported. Three different tomographic systems were developed and tested.

PACS 81.70.Tx – Computed tomography.  
PACS 87.59.-e – X-ray imaging.  
PACS 87.59.Jq – Transmission imaging.

### 1. – Introduction

X-ray Tomography (XRT) was developed around the seventies by A. M. McCormack and G. Hounsfield, who shared the Nobel prize for Medicine in 1979.

First intended for medical diagnosis, the use of XRT rapidly extended to other sectors, finding application in several non-destructive testing areas ranging from industry, to soil physics, to archaeometry [1-10].

In the field of archaeometry, this technique is better known, for example, for its visualization of the internal structure of a sample of ancient Egyptian mummies [5], but it has also been applied to ceramics and statue analysis [6-8] and restoration quality estimates [5,9].

In principle, X-ray (Transmission) Tomography consists of a large number of attenuation measurements of the radiation through a sample with a collimated beam of X- or gamma-rays crossing a section of the sample in various positions. This is obtained by moving the sample (rotating and/or translating). Transmission tomography is just a comparison between the number of collected photons, with and without the sample, and is expressed, for a well-collimated and monoenergetic beam, by the well-known

Lambert-Beer equation

$$(1) \quad I = I_0 e^{-\int_d \mu(\vec{x}, E) d\vec{x}},$$

where  $I$  is the detected intensity;  $I_0$  is the detected intensity without the sample;  $\mu(\vec{x}, E)$  is the linear attenuation coefficient which depends on the beam energy and sample composition;  $d$  is the path of the X-ray beam from the source to the detector.

After a mathematical process called “reconstruction” based on the inversion of a mathematical theorem called “Radon transform”, the distribution of the linear attenuation coefficient inside the sample is obtained.

Transmission tomography, the type of tomography normally used, is related to photons crossing the sample without interacting with it. But also photons interacting with the sample (more specifically with electrons and atoms of the sample) may be considered when obtaining tomographic images. In fact, incident photons interact with the sample with the following effects:

- photoelectric effect; an incident photon “disappears”: its energy is transferred to an internal electron of an atom of the sample which is consequently ejected. A secondary photon (fluorescent photon) is then emitted by the atom, the energy of which is characteristic of the involved element.
- Compton effect; an incident photon interacts with a electron of an atom, transferring energy and is deflected from its original direction.
- Coherent scattering (also called elastic or Rayleigh); an incident photon interacts with an atom of the sample and is deflected with the same initial energy.

The first effect can originate an X-ray fluorescence tomography (also called X-ray microscopy), which has the peculiarity of being a specific spatial map of concentration of a single element. The Compton scattered photons can also originate a tomographic image, which is much more sensitive than transmission tomography to density differences [10,11]. The coherent scattered photons are peaked in the forward direction, and their collection at small angles can originate a tomographic image, which is sensitive to atomic number differences [10].

However, each of these alternative tomographic techniques has the drawback with respect to transmission tomography, of low statistics and often require self-absorption corrections [12-14]. Transmission tomography remains, therefore, the most applied imaging technique. However, in some cases, Compton tomography can give better results [11]. X-ray fluorescence tomography, on the other hand, is limited to a few cases, but can be very significant. For example, it has been used for the determination of chemical contents in biological samples [15-17].

With reference to the possible applications of tomographic methods in the study of works of art, the main complication in this field is the variety of problems in comparison with the medical problem. In fact, in this latter field the “object” is more or less always the same, with the same composition, and, therefore, with a similar attenuation coefficient. The human body can be smaller or bigger, slim or fat, but “the material” is the same. On the contrary, works of art that are studied by tomographic methods often present not only a variety of sizes, but also variations in atomic number or density. Examples range from a piece of wood, to a column of marble, to a statue of bronze, to an object of gold, to a ceramic artefact. In this paper three different kinds of tomographic scanners are described and analysed with respect to their performance in archaeometrical studies. They differ in the detector used, which also determines the scan modality and performance.

## 2. – Methods

### a) *Tomographic systems*

Three experimental set-ups were used, all of which were developed at the University of Sassari. Two of them are based on a “matrix detector”: one on an image intensifier amplifier (IIR) and the other on a flat panel. The third apparatus is quite different and is based on a scintillation detector collimated by a cylindrical brass collimator (collimation of 1 mm).

Only one X-ray tube operating at the same experimental conditions (80 kVp and a 5 mA of continuous current) was used for all the systems. The sample was placed on a rotation-translation system.

A parallel beam was used for the area detector-based scanner. In this case, spatial resolution is determined by the size of the pixel. The spatial resolution of the detector can be artificially improved by using a cone beam illumination. In the latter case the sample is placed at a distance from the detector. As a consequence, the X-ray image size of the sample projected on the detector will be larger than the true one. This means that 4 more pixels compared to the parallel beam modality will be involved by the same volume. This approach, which is obtainable only with a microfocus tube, due to its magnification, reduces the maximum allowed size of the sample. Moreover the current of this kind of source is too low, so longer measurement time is required. Finally with cone-beam illumination, the position of the sample with respect to both the X-ray source and the detector must be carefully determined. For all these reasons we used a parallel beam approach.

The scanner based on the image intensifier can analyze samples up to 15 cm in diameter. It is attached to a ccd camera by two interchangeable custom optical systems with different magnification. The analogic signal from the ccd camera is converted to a digital form by a DT3155 acquisition board. Each radiograph is formed by  $512 \times 512$  pixels with 8 bits of dynamics (256 different levels). The spatial resolution ranges from  $300 \mu\text{m}$  to  $600 \mu\text{m}$  depending on the optical system used. These resolutions are comparable to those obtainable with high-resolution medical tomographic equipment. For the measurements reported here, only the rotation stage was used. Larger samples might be analyzed using X-rays of higher energy and/or when the samples are made of low-absorption materials. However, a maximum of about 100 keV is the upper limit of detection of this system.

In the case of tomography using the flat-panel system, it is possible to analyze samples of up to 5 cm without translating the sample. The image (radiography) acquired has  $1024 \times 1024$  pixels and a spatial resolution of  $50 \mu\text{m}$ . The maximum detectable energy is about 100 keV. The signal from the detector is acquired by an IMAQ PCI-1424 card by National Instruments. The dynamic range of CMOS array is of about 2000 different levels (about 11 bits), excluding the noise signal that takes up about 700 levels [18].

The single-detector scanner is based on a typical nuclear detection system made up of a detector, a power supply and an amplifier. The analogic signal is acquired by using a Multichannel Analyzer (MCA).

### b) *Reconstruction algorithms*

Two reconstruction algorithms were used here: filtered backprojection and FFT (Fast Fourier Transform) [19]. The quality of the reconstructed image is the same for the two algorithms. However, the FFT-based reconstruction algorithm is at least one order faster than the filtered backprojection. No quantitative calibration was performed on the measurements reported here. This is because a quantitative determination is not usually required in this kind of tomography. Usually it is more important to localize damaged areas and junctions of different materials, for example. In principle quantitative results

could be obtained by calibration with known materials as happens in medical tomography. However, the wide range of different materials involved in cultural-heritage samples makes this operation more difficult.

c) *Artifacts correction*

The data obtained by the tomographic systems described above are subject to artifacts. Therefore, before starting the reconstruction process, it is mandatory to correct them. The kind and origin of the artifact depend on both the detector and the X-ray source. They can be summarized in the following list: X-ray flux fluctuations, energy-dependent sensitivity, different responses of pixels (in the case of use of array or matrix detectors), and non-homogeneities of the X-ray illumination. In the case of the IIR detector, also distortion of the image, due to the curved surface of the detector and to magnetic fields, is observed. However, if the central part of the IIR detector is used, the spatial distortion is negligible.

The flux variations could be controlled by taking several acquisitions of the flux during the scan. The dependence on the energy of the response of the detector can be obtained by calibration. The latter is routine in a nuclear laboratory, so we do not describe it here. Regarding the other two sources of error, they require a set of calibration measurements before starting the tomographic measurement. The correction for non-homogeneity of the flux is based on the flat-field technique. Let us consider a matrix detector and let us illuminate it with the same flux used for the measurement but without the sample. The image obtained is called flat field, because it should have the same intensity at each position. However, a real flat-field image of the detector is not uniform because it contains both the spatial variation of the flux on the surface of the detector as well as the non-homogeneities of the pixel sensitivity and so it can be used for a correction procedure. The correction procedure also requires an acquisition of an image without flux (dark field). The latter enables us to remove the background produced by the detector from the flat-field measurements. After that, the mean value of the flat-field matrix is calculated. As a consequence, there will be pixels with response (value) higher than the mean value as well as pixels with a lower response. This matrix can be used for normalizing the response. In summary,

$$\text{Flat-field correction: } C(x, y) = \frac{F(x, y) - B(x, y)}{\text{mean value}},$$

where  $(x, y)$  is the spatial position of the pixel,  $F$  is the flat-field value at each position,  $B$  is the background at each pixel, mean is the mean value of the numerator.

Thus the corrected pixel response  $R$  will be given by

$$R(x, y) = \frac{R_{\text{unc}}(x, y)}{C(x, y)},$$

where  $R_{\text{unc}}$  is the uncorrected response. It is good practice to calculate  $R$  for various intensities, because of the possible non-linearity of the response of each pixel. The flat-field correction does not work for defect pixels or lines, *i.e.* pixel or line with response fixed to a wrong value; for example, zero or the maximum possible value.

In fig. 1 the uncorrected response of the matrix detector used here, a Hamamatsu C-7921CA-02 [18] is reported. In order to make the effect of spatial disomogeneity of the X-ray beam more visible, a stronger dishomogeneity of the illumination than the real one was also experimentally induced by placing the detector nearer than the real position to the X-ray tube and is visible in the top left-hand corner of fig. 1. This detector also has

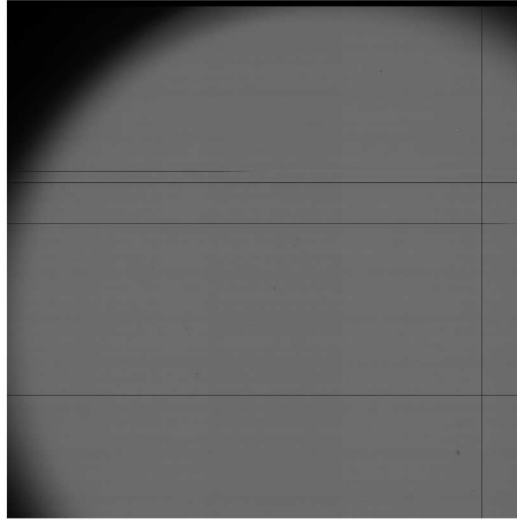


Fig. 1. – Image of the response of the detector to a flat-field illumination. The spatial variation of the X-ray beam was experimentally enhanced by placing the detector near to the X-ray source reducing the radius of the illumination cone. Five defect lines are visible.

defect lines. In order to correct the wrong value of these lines, the mean value of the two nearest working lines was used. This is possible because this detector does not have adjacent broken lines. Otherwise, a higher order or other kinds of interpolation must be used.

### 3. – Results

In this section the performances of the three systems are analyzed and compared. In fig. 2a three tomographic measurements of a nuragic vase are shown (clay vase from Sardinia, Italy, dated about 2000 years BC). The tomography was carried out using the single-detector system. The measurement time is about one day and spatial resolution is about 1 mm, *i.e.* the size of the hole of brass collimator. Higher spatial resolution can be obtained by increasing the collimation, but the measurement time will increase with the square power of the collimation radius making the measurement time too long. Moreover, the stability of the X-ray tube over such a long time cannot always be guaranteed. Depending on the acquisition time selected, flux changes can be observed even inside a single projection, making corrections difficult to perform.

In fig. 2b one slice of the set of reconstructions obtained by using the IIR as a detector are reported. This detector, as well as the flat panel, allow one to obtain a simultaneous measurement of several transversal sections (512 with the IIR and 1012 with the flat panel). The quality of the reconstructions with the IIR appears to be lower than that of the reconstruction obtained with a single detector. However, it is not completely true. In fact, the inner side of the vase appears to be more definite than in single-detector measurement and some cracks are visible. At the same time the three small handles have sharper borders in the single-detector measurement. The first behavior (spatial structures more visible) can be explained by the higher resolution of the IIR and the second, by the lower scattering obtained with the collimated single detector.

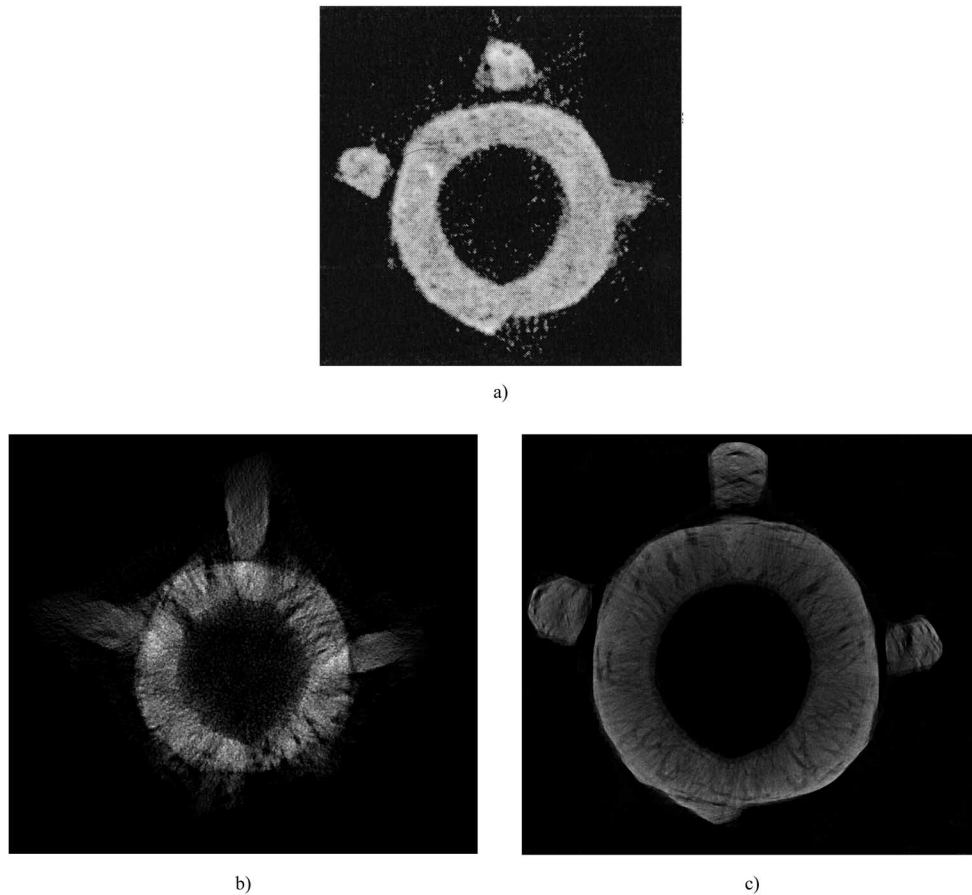


Fig. 2. – Reconstruction of a section of a nuragic vase. a) Single-detector tomograph; b) IIR tomograph and c) flat-panel tomograph.

In fig. 2c the reconstruction of approximately the same slice of fig. 2b is shown. In this case the flat-panel system was used. Due to the size of the sample (diameter of about 9 cm) a translation of the detector was required. Thus, each projection is formed by the composition of two images. The spatial resolution obtained in the latter case is higher than in the two other reconstructions and the influence of scattering appears to be lower than in the IIR measurements, probably owing to the shape of the detector surface.

It must be noted that in both the area detector systems the quality of reconstruction can be improved by raising the number of projections, maintaining acceptable measurement time.

Since stones are a material often used in cultural heritage we report here two more examples of applications of XRT to this material.

In fig. 3a reconstruction of a cylindrical section of a yellow tuff is reported. In fig. 3a the measurement was performed using a single detector while a flat panel was used in fig. 3b. Even in this case the spatial reconstruction and the quality of the image is considerably higher in the flat-panel measurement and the effect of the scattering negligible.

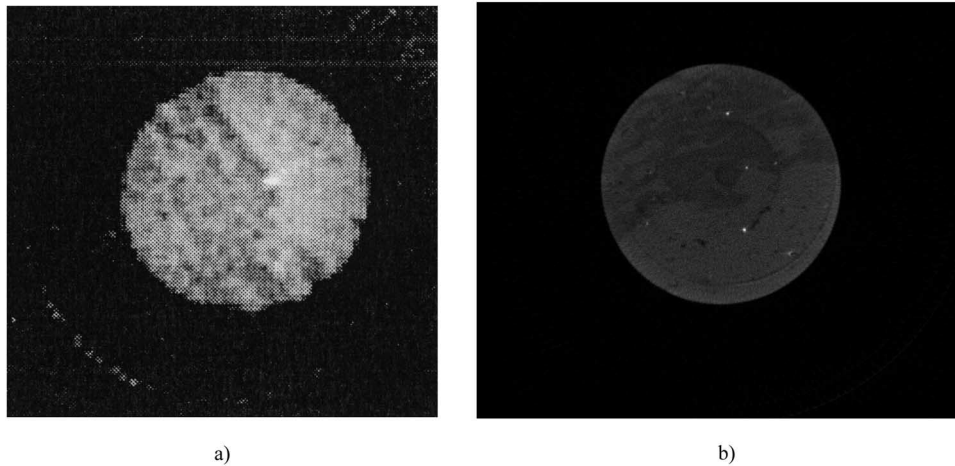


Fig. 3. – Reconstruction of a section of a tuff cylinder. a) Single-detector tomograph; b) flat-panel tomograph.

In fig. 4 the tomographic measurement is applied to estimate the penetration of a polymeric consolidant inside a stone sample. The sample size is  $5 \times 5 \times 2 \text{ cm}^3$ . In the upper and lower part of this figure the stone is shown before and after the polymeric treatment, respectively. This measurement is important because the polymeric materials are commonly used as consolidant material for stone and wood [9, 20] and the depth of penetration gives an estimate of the quality of consolidation. The system used is based on

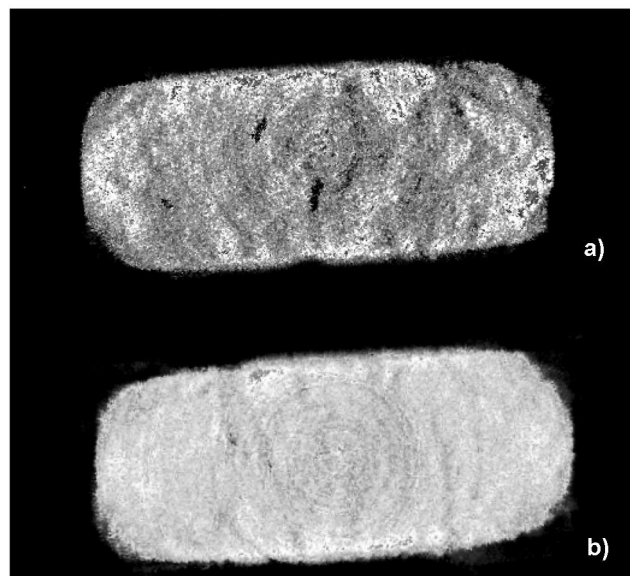


Fig. 4. – Effect of polymeric filling of a porous stone. a) Non-treated sample; b) filled sample. A IIR detector was used.

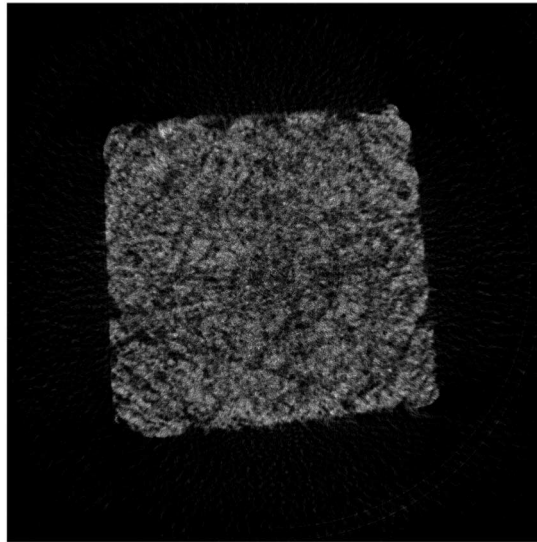


Fig. 5. – Visualization of the pores structure of a tuff called “Pietra leccese”. A flat-panel tomograph was used.

IIR detector. In order to improve and highlight the spatial resolution, thus pointing out the pore structure, the flat panel can be used as shown in fig. 5, where a “Pietra leccese” stone is reported. This kind of tuff is used in many baroque buildings in several cities in Southern Italy. The sample analyzed here is a cube of 2 cm side. The pores are clearly visible and their structures might be analyzed by using all the sets of reconstruction.

#### 4. – Discussion and conclusions

In this paper the application of different XRT systems to cultural heritage is discussed. The technical requirements and performance of three different tomographic systems have been analyzed in detail and compared. The systems based on matrix detector do not use collimators and so the amount of scattering processes recorded will be higher than with systems based on the single detector with high collimation. Thus, the best performance in terms of contrast will be obtained with the latter detector, but the high measurement time required makes this kind of apparatus practically useless. Therefore, the best alternative when considering both the quality of reconstruction and the measurement time required is a tomograph based on a flat-panel matrix. In this case a spatial resolution of up to 50 microns can be obtained and thousands of slices can be measured simultaneously. The system used in the present work is based on a C-Mos flat panel. This detector does not require cooling and the tomographic equipment easier to use and cheaper. In theory, it should be possible to design and construct a portable tomographic system based on this kind of detector. This possibility represents our future task.

#### REFERENCES

- [1] DE OLIVEIRA L. F., LOPES R. T., DE JESUS D. and BRAZ E. F. O., *Nucl. Instrum. Methods Phys. Res. A*, **505** (2003) 573.
- [2] CESAREO R. *et al.*, *Proc. SPIE*, **3772** (1999) 292.



- [3] BRAZ D., DA MOTTA L. M. G. and LOPEZ R. T., *Appl. Radiat. Isot.*, **50** (1999) 661.
- [4] IOVEA M., GEORGESCU GH., RIZESCU C. and CHITESCU P., *Non-Destr. Test. Ultrasonics*, **4**, no. 7 (1999).
- [5] JACOBS P. and CNUUDE V., in *Cultural Heritage Conservation and Environmental Impact assessment by Non-Destructive Testing and Micro-Analysis*, edited by VAN GRIEKEN R. and JANSSENS K. (Taylor & Francis Group, London) 2005.
- [6] JANSEN R. J., POULUS M., TACONIS W. and STOKER J., *Comput. Med. Imaging Graphics*, **26** (2002) 211.
- [7] ROEMICH H., LOPEZ E., MEES F., JACOBS P., CORNELIS E., VAN DICK D. and DOMENECH CARBÒ T., in *Cultural Heritage Conservation and Environmental Impact assessment by Non-Destructive Testing and Micro-Analysis*, edited by VAN GRIEKEN R. and JANSSENS K. (Taylor & Francis Group, London) 2005.
- [8] ROSSI M., CASALI F., CHIRCO P., MORIGI M. P., NAVA E., QUERZOLA E. and ZANARINI M., *IEEE Trans. Nucl. Sci.*, **46** (1999) 897.
- [9] BRUNETTI A., PRINCI E., VICINI S., PINCIN S., BIDALI S. and MARIANI A., *Nucl. Instrum. Methods Phys. Res. B*, **222** (2004) 235.
- [10] GOLOSIO B., SIMIONOVICI A., SOMOGYI A., LEMELLE L., CHUKALINA M. and BRUNETTI A., *J. Appl. Phys.*, **94** (2004) 145.
- [11] BRUNETTI A., CESAREO R., GOLOSIO B., LUCIANO P. and RUGGERO A., *Nucl. Instrum. Methods Phys. Res. B*, **196** (2002) 161.
- [12] GOLOSIO B., BRUNETTI A. and CESAREO R., *Nucl. Instrum. Methods Phys. Res. B*, **213** (2004) 108.
- [13] BRUNETTI A. and GOLOSIO B., *Comput. Phys. Commun.*, **141** (2001) 412.
- [14] BRUNETTI A., GOLOSIO B. and CESAREO R., *X-ray Spectrom.*, **31** (2002) 377.
- [15] CESAREO R. and MASCARENHAS, *Nucl. Instrum. Methods Phys. Res. A*, **277** (1989) 669.
- [16] SIMIONOVICI A., CHUKALINA M., GUNZLER F. G., SCHROER CH., SNIGIREV A., SNIGIREVA I., TUMMLER J. T. and WEITKAMP T., *Nucl. Instrum. Methods Phys. Res. A*, **467-468** (2001) 889.
- [17] SCHROER CH. *et al.*, *Proc. SPIE*, **4503** (2001) 230.
- [18] C-7921CA-02 data sheets, Hamamatsu Photonics K.K.
- [19] KAK A. C. and SLANEY M., *Principles of Computerized Tomographic Imaging* (IEEE Press, N.Y., USA) 1999.
- [20] BRUNETTI A., MARIANI A. and BIDALI S., submitted to *Nucl. Instrum. Methods Phys. Res. B*.